SELF-CONSISTENT TIGHT-BINDING APPROXIMATION INCLUDING POLARISABLE IONS

M.W. FINNIS, A.T. PAXTON, M. METHFESSEL† and M van SCHILFGAARDE‡
Department of Pure and Applied Physics, Queen's University, Belfast, BT7 1NN, UK
†Institute for Semiconductor Physics, Walter-Korsing-Str. 2
D–15230, Frankfurt (Oder), Germany
‡SRI International, Menlo Park, California 94025, USA

ABSTRACT

Until recently, tight-binding has been applied to either covalent or metallic solid state systems, or charge transfer treated in a simple point charge framework. We present a self-consistent tight-binding model which, for the first time, includes electrostatic ion polarisability and crystal field splitting. The tight-binding eigenvectors are used to construct multipole moments of the ionic charges which are used to obtain angular momentum components of the electrostatic potential in structure constant expansions. Our first test of the model is to study the phase stability in zirconia; in particular the instability of the fluorite phase to a spontaneous symmetry breaking, and its interpretation in terms of band effects and ion polarisability. This new formalism opens up the way to apply the tight-binding approximation to problems in which *polarisation* of atomic charges is important, for example oxides and other ceramic materials and surfaces of metals.

INTRODUCTION

Although the tight-binding approximation was originally conceived to deal with homopolar covalently bonded solids, an extension to include charge transfer in alloys and heteropolar semiconductors was proposed by Falicov and by Harrison some 15–20 years ago [1,2]. This self-consistent solution was extended and used very effectively by Majewski and Vogl to describe the energetics of ionically *sp*-bonded compounds [3]. A self-consistent scheme for metals has also been used [4], which in its simplest form assumes local charge neutrality [5] and leads to the tight-binding bond model [6]. Recently some questions have arisen that have motivated us to extend the self-consistent tight-binding approximation with charge transfer to include the effects of polarisation of the atomic charges. Such observations include,

1. The electronic structure of a low coverage of Nb on the (0001) α-Al_2O_3 surface has been observed to have the character of a single non degenerate *d*-orbital. We found it impossible to describe this with conventional orthogonal or non orthogonal tight-binding, in which the on site hamiltonian matrix elements are constrained to be the same for each angular momentum (*ie*, crystal field splitting is ignored).
2. There is a question whether surface dipole barriers and hence work functions could be calculated in the tight-binding approximation.
3. It is thought that the spontaneous distortion of cubic zirconia into the tetragonal structure is driven by the quadrupole polarisability of the oxygen atoms [7].
4. One would like to include crystal field terms as a natural consequence of the non spherical Madelung potential, rather than by direct parameterisation as has been done previously [8].

Mat. Res. Soc. Symp. Proc. Vol. 491 © 1998 Materials Research Society

THEORY

Traditional self-consistent tight-binding

In order to make our new approach clear we begin with a brief reminder of Harrison's scheme which will also serve to establish our notation. In non self-consistent tight-binding, one supposes the existence of a hamiltonian $\mathcal{H}_0$ whose matrix elements between localised (not necessarily orthogonal) basis functions are $\langle \mathbf{R}' L' | \mathcal{H}_0 | \mathbf{R} L \rangle$. Although the basis functions are never specified, without loss of generality one may write them as a radial part times an angular part:

$$|\mathbf{R}L\rangle = f_{\mathbf{R}\ell}(|\mathbf{r} - \mathbf{R}|) Y_L(\mathbf{r} - \mathbf{R}). \tag{1}$$

Here we use $\mathbf{R}$, $\mathbf{R}'$ to denote the position of atomic sites with respect to some origin. To simplify the equations, we will frequently suppress the site index, in which case one can take it that we are referring to an atom at the origin and $\mathbf{r}$ is a small vector in its neighbourhood. L is a composite angular momentum index $L = \{\ell m\}$ and Y_L is a real spherical harmonic [9].

In the traditional self-consistent approach, having solved Schrödinger's equation, the eigenvectors are used to determine to what extent charge has been redistributed among the atoms. There will be a charge

$$q = Q_0 Y_0 = \mathrm{e} \sum_{\ell} N_\ell$$

on each site, where Q_0 is the monopole moment of the charge, N_ℓ is the Mulliken population of angular momentum ℓ (s, p and d) and e is the charge on the electron. The hamiltonian is adjusted self-consistently to become $\mathcal{H} = \mathcal{H}_0 + \mathcal{H}'$ where $\mathcal{H}'$ *is diagonal* in $\mathbf{R}L$:

$$\mathcal{H}'_{\mathbf{R}L\mathbf{R}L} = \mathrm{e} V_{\mathbf{R}0} + U_{\mathbf{R}\ell} N_{\mathbf{R}\ell}. \tag{2}$$

Here, $V_{\mathbf{R}0}$ is the $\ell = 0$ component of the electrostatic potential at site $\mathbf{R}$ due to the charges at all other sites, and $U_{\mathbf{R}\ell}$, sometimes called the "Hubbard U" is a positive energy which resists the accumulation of charge. The physical meaning of U in this context is discussed in detail by Harrison [2]. The benefit of this model which goes beyond non self-consistent tight-binding is that one can treat mixed ionic–covalent solids with real success [3].

Self-consistent tight-binding with multipoles

What is missing, and what is added in our new formulation here, is any adjustment of the *off-diagonal* on-site matrix elements of $\mathcal{H}'$. These matrix elements couple orbitals of different angular momenta, ℓ and m, on the same site. One effect this can have is to break the degeneracy of the s, p and d orbital energies, and thereby induce effects such as crystal field splitting or phenomena such as that mentioned as item 1 in the introduction. Furthermore, these new matrix elements lead to *polarisability* of the ionic valence electrons. One could then study, for example, polarisable anion theories of oxide structure and lattice dynamics, or phenomena such as lattice instability and ferroelectricity. What couple these orbitals on the same site are the higher angular momentum components of the electrostatic potential. In fact we may regard V_0 in (2) as just the coefficient of the first term in an expansion in spherical waves of the electrostatic potential at a point $\mathbf{r}$ near an atom at the origin:

$$V(\mathbf{r}) = \sum_{L} V_L \, r^\ell \, Y_L(\mathbf{r}). \tag{3}$$

For $\ell = 1$ and $\ell = 2$ respectively, V_L are proportional to the electric fields and field gradients at the nucleus [9]. It is the $\ell = 4$ components of V_L that are responsible for the splitting of the d levels by cubic, octahedral or tetrahedral crystal fields in transition metal oxides [10].

In a similar vein we would expect the charge on each atom to have not only $l = 0$ components as in (2), but higher multipole moments, which would be

$$\begin{aligned} Q_L &= \mathrm{e}\int \mathrm{d}\mathbf{r}\rho(\mathbf{r})r^\ell Y_L(\mathbf{r}) + q^{\mathrm{c}}Y_0\delta_{L0} \\ &= Q_L^{\mathrm{e}} + Q^{\mathrm{c}}\delta_{L0} \end{aligned} \tag{4}$$

if we knew the electronic charge density $\mathrm{e}\rho(\mathbf{r})$ associated with each atom. We have included here $Q^{\mathrm{c}} = q^{\mathrm{c}}Y_0$ which is the monopole moment of the core charge q^{c}, and in the second line have separated the total charge into a part from the valence electrons and a part from the ion cores. If we assume the charges are sufficiently localised about their atomic sites, we can find a relation for the components of the electrostatic potential $V_{\mathbf{R}L}$ on one site, due the multipole moments of the charges on all other sites. Using Poisson's equation and an expansion in the structure constants of LMTO-ASA theory, we find

$$V_{\mathbf{R}L} = 4\pi \sum_{\mathbf{R}'\neq\mathbf{R}} \sum_{L'} \bar{B}_{LL'}(\mathbf{R}' - \mathbf{R})\, Q_{\mathbf{R}'L'}.$$

The structure constants are [11,12]

$$\tilde{B}_{LL'}(\mathbf{R}) = 4\pi \sum_{L''}{}' \frac{(2\ell''-1)!!}{(2\ell+1)!!(2\ell'+1)!!} \left(\frac{1}{R^{\ell''+1}}\right)(-1)^{\ell'} Y_{L''}(\mathbf{R})\, C_{L''L'L}$$

(with the sum over L'' restricted to values for which $\ell'' = \ell + \ell'$) and

$$C_{L''L'L} = \int \mathrm{d}\Omega\, Y_{L''}\, Y_{L'}\, Y_L \tag{5}$$

are Gaunt coefficients for real spherical harmonics. The sum over $\mathbf{R}'$ is done by the Ewald method.

From eigenvectors to total energy, and some new parameters

Although the charge density is not calculated in an empirical tight-binding model, we can nevertheless obtain the multipole moments (4) in the following way. Equation (4) demonstrates that Q_L^{e} is the expectation value of a certain function of the position operator $\hat{\mathbf{r}}$, namely [9]

$$\hat{Q}_L^{\mathrm{e}} = \mathrm{e}\,\hat{r}^\ell\, Y_L(\hat{\mathbf{r}}). \tag{6}$$

Now, a tight binding calculation normally provides eigenvectors for each band index n and wavevector $\mathbf{k}$, $c_{\mathbf{R}L}^{n\mathbf{k}}$, from which one obtains the charges on each site. We can use these to obtain also the multipole moments as the expectation value of the operator $\hat{Q}_L^{\mathrm{e}}$:

$$Q_L^{\mathrm{e}} = \sum_{L'L''} \sum_{\substack{\mathrm{occ.}\\ n\mathbf{k}}} \bar{c}_{L'}^{n\mathbf{k}} c_{L''}^{n\mathbf{k}} \langle L'|\hat{Q}_L^{\mathrm{e}}|L''\rangle. \tag{7a}$$

We can now use (1), (5) and (6) to express the matrix elements of $\hat{Q}_L^{\mathrm{e}}$ as

$$\langle L'|\hat{Q}_L^{\mathrm{e}}|L''\rangle = \mathrm{e}\,\Delta_{\ell'\ell''\ell}\, C_{L'L''L}. \tag{7b}$$

Included in (7) are important quantities $\Delta_{\ell'\ell''\ell}$ which will be introduced as new parameters of the empirical tight binding model:

$$\Delta_{\ell'\ell''\ell} = \int r^2 \mathrm{d}r f_{\ell'}(r) f_{\ell''}(r) r^{\ell}.$$

In the case that $\ell' = \ell''$ these are parameters $\langle r^{\ell} \rangle$ already familiar from crystal field theory [10].

There is only a limited number of new "Δ-parameters" due to selection rules and symmetries of the $C_{L'L''L}$ and the $\Delta_{\ell'\ell''\ell}$. Also $\Delta_{\ell\ell'0} = \Delta_{\ell\ell 0}\delta_{\ell\ell'}$ and is determined by the normalisation of (1). The new parameters that will have to be determined (for a tight binding basis up to $\ell = 2$) are

$$\begin{aligned}
\Delta_{011} = \Delta_{101} &\equiv \Delta_{spp} \\
\Delta_{112} &\equiv \Delta_{ppd} \\
\Delta_{022} = \Delta_{202} &\equiv \Delta_{sdd} \\
\Delta_{121} = \Delta_{211} &\equiv \Delta_{pdp} \\
\Delta_{222} &\equiv \Delta_{ddd} \\
\Delta_{123} = \Delta_{213} &\equiv \Delta_{pdf} \\
\Delta_{224} &\equiv \Delta_{ddg}.
\end{aligned}$$

The physical meaning of these parameters in the context of equation (7) is as follows. Occupied orbitals of angular momentum (s, p or d-type) ℓ' and ℓ'' combine to produce a multipole moment on the same site of angular momentum ℓ. The strength of the multipole is proportional to the size of $\Delta_{\ell'\ell''\ell}$ and the Gaunt coefficients dictate the selection rules.

The next step is to construct matrix elements of $\mathcal{H}'$. This is done in much the same way as in making matrix elements of $\hat{Q}^{\mathrm{e}}_L$ since $V(\mathbf{r})$ is also expanded in r^{ℓ}. (Compare equations (3) and (6).) We therefore obtain

$$\mathcal{H}'_{\mathbf{R}L'\mathbf{R}L''} = \mathrm{e}\sum_L V_{\mathbf{R}L}\,\Delta_{\ell'\ell''\ell}\,C_{L'L''L} + U_{\mathbf{R}\ell'}N_{\mathbf{R}\ell'}\,\delta_{L'L''} \tag{8}$$

in analogy with equation (2), in which, perhaps not surprisingly, the $\Delta_{\ell'\ell''\ell}$ appear for a second time. In this context their physical interpretation is that multipoles on all other sites have induced a potential on a particular site. The ℓ-component of that potential then causes a coupling in $\mathcal{H}'$ between ℓ' and ℓ'' orbitals on that site. The quantity $\Delta_{\ell'\ell''\ell}$ describes the strength of that coupling. This is essentially the same explanation as in the previous paragraph but viewed from different standpoint. Drawing again on the example of crystal field splitting in transition metal oxides, the $\ell = 4$ component of the potential on the transition metal nucleus, due to the surrounding oxygen neighbours, causes a coupling between the d-orbitals which breaks their degeneracy. The strength of this coupling (called the cubic field splitting, Δ [10]) is proportional to the integral $\Delta_{ddg} = \langle r^4 \rangle$.

We can complete our model, finally, by working out the total energy. In conventional non self-consistent tight-binding, the total energy, E_{T}, contains two terms: the sum of one electron eigenvalues, E_{band} and a repulsive pair-wise potential energy E_{pair} [13]. In our case since we are including the total (core plus valence) charge, and since the electron–electron interaction

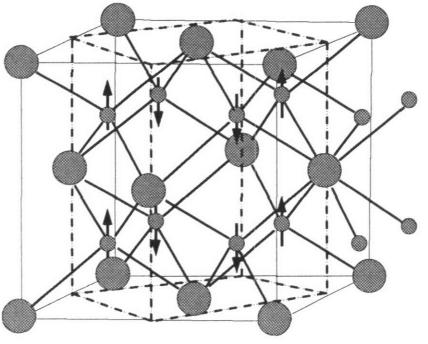

FIG 1: Atomic positions in the fluorite and tetragonal modifications of ZrO_2. Large circles are Zr atoms and small circles oxygen. Arrows represent the displacements of the columns of oxygen atoms that cause the spontaneous transition from cubic to tetragonal ZrO_2. A broken line outlines a unit cell of tetragonal ZrO_2. In the present model calculations we retain the cubic lattice constant so that the axial ratio of the tetragonal phase is constrained at $\sqrt{2}$.

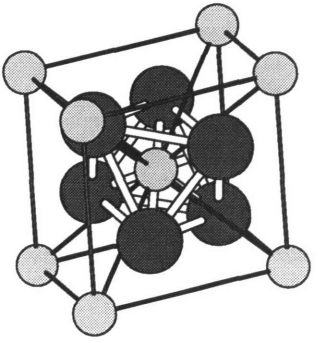

FIG 2: Atomic structure of the rutile phase. Here the small atoms are Zr. Note how whereas in fluorite (as seen on the right of fig 1) the transition metal atom is in the centre of a cube *of anions, in rutile the transition metal atom is in an* octahedral *crystal field, which reverses the order of the t_2 and e sub band energy levels (see fig 4).*

will be double counted in E_{band}, we will need to add two further terms, the ion-ion repulsive electrostatic energy, E_{ii}, and the double counting correction $-E_{\text{DC}}$. We find

$$\begin{aligned} E_{\text{T}} &= E_{\text{band}} + E_{\text{pair}} + E_{\text{ii}} - E_{\text{DC}} \\ &= \langle \mathcal{H} \rangle + E_{\text{pair}} + \frac{1}{2} \text{e} \sum_{\mathbf{R}} Q^{\text{c}}_{\mathbf{R}} V_{\mathbf{R}0} - \frac{1}{2} \text{e} \sum_{\mathbf{R}L} Q^{\text{e}}_{\mathbf{R}L} V_{\mathbf{R}L} - \frac{1}{2} \sum_{\mathbf{R}\ell} U_{\mathbf{R}\ell} N^2_{\mathbf{R}\ell}. \end{aligned}$$

Using $\langle \cdots \rangle$ we have written the usual band energy as the expectation value with respect to the self consistent one electron eigenvectors of the hamiltonian $\mathcal{H}$. We may obtain an exact derivative of E_{T} in order to calculate the interatomic forces. This is a generalisation of the expression due to Sutton *et al.* [6] since we include a finite U. Omitting small dipole–dipole and dipole–higher-multipole terms (which can be written down explicitly) we find, for the z-component of the force on an atom at the origin,

$$F_z = -2 \left\langle \frac{\partial \mathcal{H}_0}{\partial z} \right\rangle - \frac{\partial E_{\text{pair}}}{\partial z} + \sqrt{\frac{3}{4\pi}}\, Q_0 V_{10}.$$

Note the first two terms are exactly the force used in non self consistent tight-binding [6,13], except the eigenvectors are self consistent. The final term accounts for the double counting (the "U" terms cancel) and V_{10} as in (3) is the $\ell = 1$ component of the potential ($m = 0$ for the z-component of the force) and Q_0 is the total charge as in (4).

APPLICATION TO PHASE STABILITY IN ZIRCONIA

In order to demonstrate the model in an example, we address the question mentioned in item 3 in the introduction, namely the phase stability in zirconia, ZrO_2. The zero temperature, ground state structure is a complex monoclinic phase. Below the melting point ZrO_2 has the fluorite structure, illustrated in fig 1; but at intermediate temperatures this structure transforms to a tetragonal phase in a spontaneous symmetry breaking also illustrated in fig 1. We will concern ourselves here with model calculations aimed at predicting this symmetry breaking. Therefore, while the phase transition is accompanied by a change in the tetragonal axial ratio, we will consider only the distortion illustrated in fig 1 and keep the lattice constant fixed at the cubic value which we choose to be 5.18Å. We are able to compare our results with *ab initio* density-functional calculations using a new, high precision, band-structure program in a basis of smooth Hankel functions augmented in atomic spheres, with plane wave expansions of the potential and charge density in interstitial regions [14]. For ZrO_2 we use nine $2s2p3d$ oxygen basis functions at kinetic energy $\kappa^2 = -0.2$Ry and a further s function at $\kappa^2 = -0.5$, augmented in spheres of radius 1.8 a.u. Zr basis functions are $5s$ at $\kappa^2 = -0.01, -0.5, -2$, $4p$ at $\kappa^2 = -0.01, -0.4, -2$ and $4d$ at $\kappa^2 = -0.1, -0.4$. The Zr $5p$ are too high in energy to contribute significantly to the energy bands and the Zr $4s$ dispersion is treated in a frozen, overlapping core approximation. The radius of the Zr atomic spheres is 2.1 a.u.

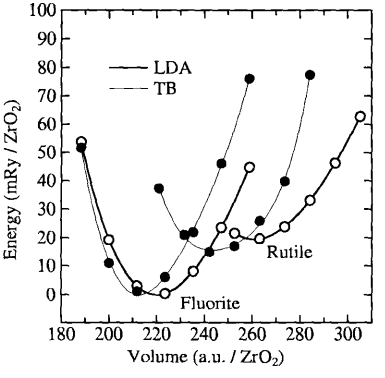

FIG 3: Energy volume curves for fluorite and rutile ZrO_2 calculated in the local density approximation (open circles) and in the new tight-binding model (filled circles). All electronic structure parameters were adjusted to reproduce the energy bands (fig 4) and so only the two parameters in the Born-Mayer repulsive potential were available to fit to the minima and curvature of the ab initio *data.*

We have attempted to make our tight-binding model for ZrO_2 as simple as possible. Therefore we employ a minimal basis of only $4d$ orbitals on Zr and $2p$ and $3s$ on oxygen. In this way we are describing only the $2p$ and not the $2s$ valence bands of oxygen and using the O–$3s$ states to describe the higher lying bands and also to mix with the $2p$ to provide the polarisability of the oxygen ion. Relative to the energy of the O–$2p$ level, the O–$3s$ atomic

level is at 0.35Ry, and the Zr–4*d* at 0.1Ry. We use a value of $U = 1$Ry on all orbitals. We allow only nearest neighbour matrix elements between oxygen atoms, namely $ss\sigma$, $sp\sigma$, $pp\sigma$, $pp\pi$ and have used length scaling adjusted to reproduce the volume dependence of the O–2*p* band width in an *ab initio* calculation. The only other inter-site matrix elements are those connecting Zr and oxygen, namely $sd\sigma$, $pd\sigma$ and $pd\pi$. These scale in the usual canonical way [11]. Only in the case of the rutile structure, shown in fig 2 do we also allow Zr-*d*–Zr-*d* matrix elements (between the two-fold coordinated Zr ions along the *c*-axis) and these are also chosen canonically. The magnitudes of the hopping matrix elements are chosen to approximately reproduce the *ab initio* band widths. The pair potential we employ is of the Born–Mayer form: $\phi(r) = Ae^{-\lambda r}$, between oxygen and Zr nearest neighbours only, and we have chosen A and λ to reproduce approximately the *ab initio* energy volume curves of ZrO_2 in the fluorite and rutile structures. These are shown in fig 3. Comparison between the tight-binding and *ab initio* energy bands are shown in fig 4. We can discuss our choices of the $\Delta_{\ell''\ell'\ell}$ parameters in terms of these.

First we mention those pertaining to the Zr sites. The most important is Δ_{ddg} and this is the integral denoted $\langle r^4 \rangle$ in crystal field theory of transition metal ions [10]. In an environment with cubic point symmetry, the first non vanishing component of the potential in the expansion (3) is for $\ell = 4$ and it is this which breaks the degeneracy of the five *d*-orbitals and splits them into the t_2 and e manifolds. In an octahedral or tetrahedral environment the t_2 states are split below the e and *vice versa* in a cubic field. Our approach incorporates this feature very naturally for a single value of Δ_{ddg} as seen in fig 4, where in fluorite the t_2 bands are higher and in rutile they are lower than the e bands. A value of $\Delta_{ddg} = 65$ a.u. achieves proper agreement between tight-binding and *ab initio* bands. The only other Δ-parameter needed is Δ_{ddd} and we find the bands quite insensitive to its choice. We set $\Delta_{ddd} \approx \sqrt{\Delta_{ddg}}$.

On the oxygen sites, in the minimal basis there are also two Δ-parameters. These are Δ_{spp} and Δ_{ppd}. In fluorite, there are no dipole or quadrupole moments on the oxygen ions and these integrals do not contribute to the bandstructure. The O-2*p* bandwidth is controlled by the magnitude of the hopping integrals. However rutile is necessarily distorted in the sense that the space group symmetry is tetragonal, while the oxygen octahedra are imperfect. Therefore there are both dipole and quadrupole moments on the oxygen sites. Whereas the bands are found to be insensitive to the value of Δ_{spp}, we find that it is Δ_{ppd} that controls the width of the O-2*p* band due to the splitting of the O-*p* levels by the field gradients. This exposes an essential difference between the fluorite and rutile modifications of ZrO_2 which emphasises the value of our model used in combination with *ab initio* band calculations. We will defer attaching a value to Δ_{spp} until the next paragraph.

The next and final question we will address is the role of the electronic structure in the spontaneous distortion of the fluorite structure to the tetragonal phase—modelled in the present work as the change in total energy along the one dimensional path as the oxygen atomic columns move alternately up and down as shown in fig 1, while keeping the lattice constants fixed. The total energy calculated *ab initio* is shown in fig 5, and this calculation predicts the same minimum as an earlier density-functional calculation using full potential LAPW [15]. Since the dipole moment arising from the symmetry breaking contributes to the amount of force on the oxygen ions, we now adjust the final Δ-parameter, Δ_{spp} on the oxygen sites to obtain as close agreement as we can with the *ab initio* energy. We see that the model correctly predicts the symmetry breaking phase transition from fluorite to the tetragonal modification.

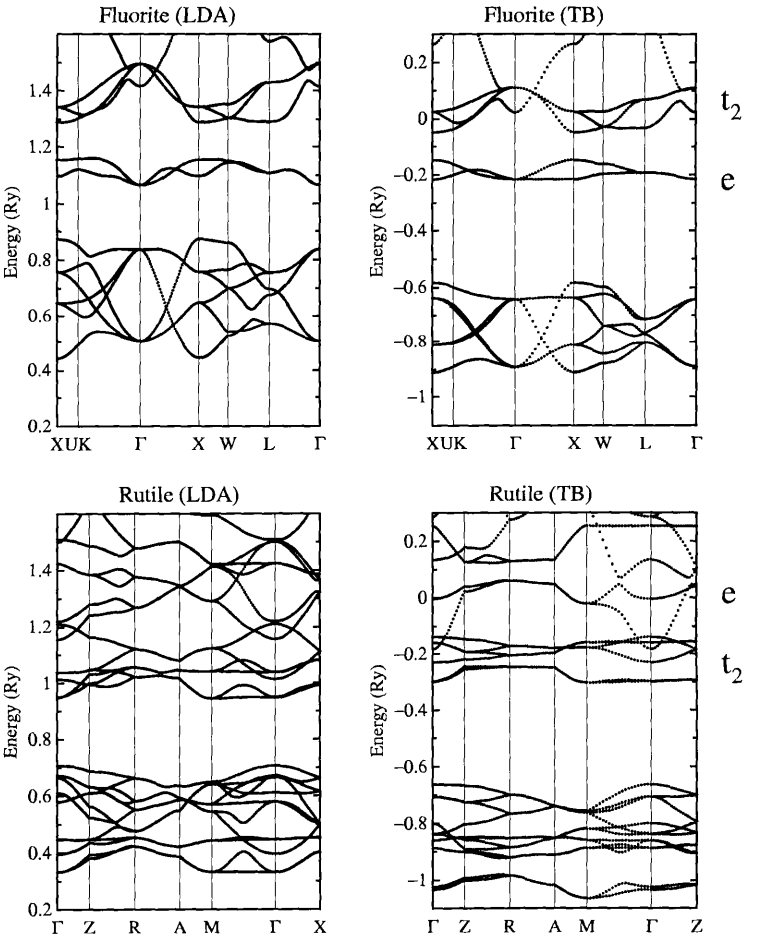

FIG 4: Energy bands in fluorite and rutile ZrO_2 using local density approximation (left) and the new tight-binding model (right). The energy zeros are arbitrary. In all four figures, the lowest lying set of bands are the occupied oxygen 2p valence bands. Unoccupied Zr 4d and oxygen 3s bands are separated from these by a band gap. Features to note are (i) the good reproduction of the fluorite LDA bands in the minimal basis tight-binding approximation. The free-electron-like parabola at Γ above and hybridised with the t_2 manifold is the oxygen 3s band; (ii) again, in fluorite, the cubic symmetry demands that the only relevant Δ-parameters are Δ_{ddd} and Δ_{ddg} on Zr. The former has little effect on the bands but it is Δ_{ddg} that produces the large crystal field splitting of the 4d bands; (iii) in rutile the sign of the cubic splitting is reversed, and this effect is reproduced naturally in our structure constant expansion without explicit fitting; (iv) whereas the width of the 2p bands in fluorite is determined by the size of the pp and pd hopping integrals, in rutile the width is largely determined by the size of Δ_{ppd} which we adjust to reproduce the LDA bandwidth.

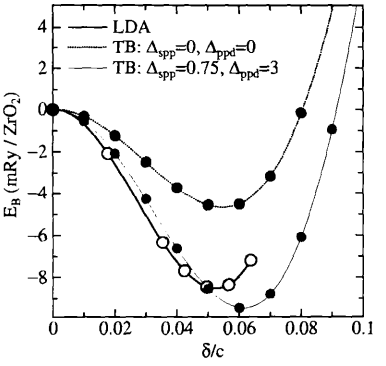

FIG 5: Energy as a function of the displacement δ of oxygen atoms in units of the tetragonal c lattice parameter (in our case equal to the fluorite lattice constant)—see fig 1. Open circles are the ab initio *LDA data. We show two sets of data from the new tight-binding model. The thin full line are data employing Δ-parameters (in a.u.) as shown. Δ_{ppd} has already been fixed to obtain the correct width of the valence band in rutile. Δ_{spp} which produces the dipole moment on the oxygen atom has been adjusted to get agreement with the LDA data here. The broken line shows the energy in the point charge self-consistent tight-binding approximation, where the Δ-parameters are set to zero. The distortion persists in this limit although the energy gain is less. This demonstrates that the distortion is not a consequence of the polarisablility of the oxygen ions alone, but that this does play a major rôle.*

DISCUSSION AND CONCLUSIONS

As far as we know, this is the first time that tight-binding theory has been extended to include polarisability and crystal field splitting by direct calculation of the charge and potential expanded in angular momentum components. With only a small number of physically motivated parameters, one may now include these effects in order to address topics such as those mentioned in the introduction. We expect there to be many more potential applications.

In the example we have chosen, we have shown firstly how a very small set of basis functions, properly chosen, is adequate to obtain the bandstructure of fluorite ZrO_2 in agreement with *ab initio* bands. By including the parameterised crystal field Δ-integrals, the Zr–4*d* bands split naturally into t_2 and *e* sub bands, and this splitting is reversed in rutile simply as a consequence of using a structure constant expansion for the potential, without the need of explicit parameterisation. Futhermore in rutile we see the importance of crystal field effects upon the width of the O–2*p* band, a fact that would be hard to deduce without working within a model such as ours to interpret *ab initio* bands. By choosing just two parameters in a simple pair potential, our model is able to reproduce the fact that the rutile structure is less stable than fluorite; consistent with rutile never being observed as a pseudomorph of ZrO_2 despite this being the stable phase of TiO_2. This competition between rutile and fluorite is problematic in many atomistic descriptions in terms of purely classical electrostatic terms, and this is a consequence of the ionic radius of Zr^{4+} placing ZrO_2 on the border between prefering six or eight-fold coordination by oxygen if one uses the usual radius ratio rules [7].

Finally the model correctly predicts the spontaneous symmetry breaking in the fluorite structure.

We can also use the results of our calculations to address the question of the *origin* of the symmetry breaking. In a non quantum mechanical description [7], the symmetry breaking introduces extra degrees of freedom, particularly the quadrupole polarisation of the oxygen ion and this allows the crystal to lower its energy. We can test this hypotheses by calculating the energy path after setting the Δ-parameters to zero (*ie*, returning to the point charge self-consistent tight-binding approximation). As seen in fig 5, the symmetry breaking persists in this limit indicating bandstructure effects at work in addition to classical electrostatic forces. However, the effect is weakened indicating the role of the ionic polarisability in the phase transition.

We expect this preliminary investigation to lead to further applications of our new formalism. Including polarisation of atomic charges in the tight-binding approximation will allow calculations of lattice dynamics and defect structure in oxides and other ceramic materials. We anticipate also applications to surface structure and defects as well as work functions in metals. A combined approach to metals and ceramics will assist in our understanding of the metal ceramic interface and the nature of bonding in such heterogeneous solid state systems. New applications in molecular physics may also be realised.

REFERENCES

1. R. C. Kittler and L. M. Falicov, *Phys. Rev. B*, **18**, 2506 (1978); M. O. Robbins and L. M. Falicov, *Phys. Rev. B*, **29**, 1333 (1984).
2. W. A. Harrison, *Phys. Rev. B*, **31**, 2121 (1985).
3. J. A. Majewski and P. Vogl, *Phys. Rev. Lett.*, **57**, 1366 (1986); *Phys. Rev. B*, **35**, 9679 (1987).
4. A. T. Paxton, *J. Phys. D*, **29**, 1689 (1996)
5. C. Priester, G. Allan and M. Lannoo, *Phys. Rev. B*, **33**, 7386 (1986).
6. A. P. Sutton, M. W. Finnis, D. G. Pettifor and Y. Ohta, *J. Phys. C*, **21**, 35 (1988)
7. M. Wilson, U. Schönberger and M. W. Finnis, *Phys. Rev. B*, **54**, 9147 (1996).
8. D. J. Chadi, in *Atomistic simulation of materials*, edited by V. Vitek and D. J. Srolovitz (Plenum Press, New York, 1989), p. 309.
9. A. J. Stone, *The theory of intermolecular forces*, (Oxford University Press, 1996).
10. J. S. Griffith, *Theory of transition metal ions*, (Cambridge University Press, 1960); D. S. McLure, in *Phonons*, edited by R. W. H. Stevenson (Oliver and Boyd, London, 1966); A. M. Stoneham, *Theory of defects in solids*, (Oxford University Press, 1975).
11. O. K. Andersen, in *NATO ASI: The electronic structure of complex systems*, edited by P. Phariseau and W. M. Temmerman, (Plenum, New York, 1984), p. 11.
12. M. Methfessel, *Multipole Green functions for electronic structure calculations*, (Katholieke Universiteit te Nijmegen, 1986).
13. D. J. Chadi, *Phys. Rev. B*, **41**, 1062 (1978)
14. M. Methfessel and M. van Schilfgaarde, *NFP Manual 1.00*, (IHP-Frankfurt/Oder, 1997).
15. H. J. F. Jansen, *Phys. Rev. B*, **43**, 7267 (1991).